Available online at www.sciencedirect.com
ScienceDirect
ELSEVIER
Optics Communications 266 (2006) 620–626
OPTICS COMMUNICATIONS
www.elsevier.com/locate/optcom

More precise determination of thermal lens focal length for end-pumped solid-state lasers

Shuzhen Fan, Xingyu Zhang *, Qingpu Wang, Shutao Li, Shuanghong Ding, Fufang Su

School of Information Science and Engineering, Shandong University, Jinan 250100, PR China

Received 29 September 2005; received in revised form 8 May 2006; accepted 9 May 2006

Abstract

A method of more precise determination of the focal length of equivalent thermal lens (TL) is presented in this paper. The method is based on the diffraction theory of aberrations. By numerically calculating the optical path difference (OPD) distribution and the Strehl ratio, the focal lengths for "top-hat" pumping and Gaussian pumping are obtained and the equations for the focal lengths are presented by curve fitting. Also the equations for average pump radii are presented. The experiment on a fiber-coupled LD pumped Nd:YAG laser is carried out. The experimental results verify the validity of the method.

Keywords: Thermal lens; Focal length; Diffraction theory of aberrations; Strehl ratio; End-pumped solid-state laser

1. Introduction

Thermal effect in the gain medium is an important factor influencing the characteristics of end-pumped solid-state lasers. A convenient way of investigating the thermal effect is to use an imaginary thermal lens (TL) with the equivalent focal length.

Koechner is one of those who first studied the thermal lens in solid-state laser rod analytically. He gave the analytical solutions and the equation of the TL focal length for uniform heating in 1970 [1]. For Gaussian distribution of the pumping beam, the expression of the TL focal length was presented by Innocenzi in 1990 [2]. This expression has been modified to include more effects by many authors and has been widely used [3–7]. Cousins studied "top-hat" pump analytically and gave the temperature distribution [8] and the optical path difference (OPD) distribution [9]. Many authors gave expressions of the TL focal length by using the quadratic part of the OPD based on Cousins' works [7,10–13]. We found that the actual TL focal length is larger than that calculated by these expressions and so did some others [14–16].

We work out the cause leading to this difference and give a revised expression of the TL focal length that is more precise. In Appendix A we provide some of the derivations in order to clarify some of the assumptions and notations used in this paper, and to derive some expressions. The expression of the focal length that is more precise is presented in part II. The expression of the average pump radius is presented in part III. In part IV, we give our experimental evidence to show that the new results are closer to the experimental results than the old ones.

2. TL focal length with average pump radius

The pump profile of a fiber-coupled LD pumped laser is usually regarded as "top-hat". As to the nonlinear crystal in OPO, Raman medium, saturable absorber or lasers pumped by other TEM_{00} mode lasers, the pump profile is usually considered as Gaussian. The most popular cooling scheme is the side cooling for it's economical and easy to set up [5]. So the boundary condition is set as copper heat sink side-cooled scheme (with or without indium foil). The

* Corresponding author. Tel.: +86 531 88362358.
E-mail address: xyz@sdu.edu.cn (X. Zhang).

0030-4018/$ - see front matter © 2006 Elsevier B.V. All rights reserved.
doi:10.1016/j.optcom.2006.05.023

temperature distribution in the crystal is given by Eqs. (A9) and (A10) (see Appendix A).

The optical path difference (OPD) theory is a bridge between the imaginary lens and the thermal effect. The OPD of an ideal lens is parabolic and is given by [17]

$$\mathrm{OPD}(r) - \mathrm{OPD}(0) = -\frac{r^2}{2f}, \tag{1}$$

where f is the focal length of the lens, r is the radial coordinates.

The thermally induced OPD is more complex. It includes the change of refractive index with temperature, the end-faces bulging out, and the stress-induced birefringence. The last one is about one tenth of the former two parts taking YAG for example and may be neglected [8,17]. Then the OPD distribution in the slice z to $z + \mathrm{d}z$ is [10]

$$\mathrm{dOPD}(r,z) = \left[\frac{\partial n}{\partial T} + (n-1)(1+\upsilon)\alpha_\mathrm{T} + 2C_\mathrm{r}n^3\alpha_\mathrm{T}\right]\Delta T(r,z)\,\mathrm{d}z, \tag{2}$$

where υ is the Poisson's ratio, α_T is the thermal expansion coefficient, n is the refractive index of the medium, C_r is the photo-elastic coefficient. Note that if the rear mirror is the coating of the rod end face, $(n-1)$ in Eq. (2) should be replaced by n.

The total optical path difference distribution $\mathrm{OPD}(r)$ could be gotten by integrating Eq. (2) over z from 0 to l, the length of the crystal. To make the integration simpler, $\omega_\mathrm{p}(z)$ is simplified as ω_pa, the average pump radius in the crystal. The relation between ω_pa and $\omega_\mathrm{p}(z)$ will be presented in part III. When considering the pump radius being constant in the crystal, ω_pa is just the waist radius of the pump beam. For simplicity, we define a parameter A_0 as

$$A_0 = \frac{\eta_\mathrm{h}P_\mathrm{abs}}{4\pi K} \times \left[\frac{\partial n}{\partial T} + (n-1)(1+\upsilon)\alpha_\mathrm{T} + 2C_\mathrm{r}n^3\alpha_\mathrm{T}\right]. \tag{3}$$

It can be seen that A_0 is related to the characteristics of the crystal and the pumping power. The total path difference distribution $\mathrm{OPD}(r)$ can be written as

$$\mathrm{OPD}(r) = A_0 \times \left\{\left[1 - \frac{r^2}{\omega_\mathrm{pa}^2} + \ln\left(\frac{r_0^2}{\omega_\mathrm{pa}^2}\right)\right]\Theta\left(\omega_\mathrm{pa}^2 - r^2\right) + \ln\left(\frac{r_0^2}{r^2}\right)\Theta\left(r^2 - \omega_\mathrm{pa}^2\right)\right\} \quad \text{(for “top-hat” pumping)}, \tag{4}$$

$$\mathrm{OPD}(r) = A_0 \times \left[\ln\left(\frac{r_0^2}{r^2}\right) + E_1\left(\frac{2r_0^2}{\omega_\mathrm{pa}^2}\right) - E_1\left(\frac{2r^2}{\omega_\mathrm{pa}^2}\right)\right] \quad \text{(for Gaussian pumping)}. \tag{5}$$

As is shown in Fig. 1, surface A is an example of the OPD in an actual crystal for “top-hat” pumping. The central part ($r < \omega_\mathrm{p}$) is just parabolic (see Fig. 1 and Eq. (4)) and the rest is logarithmic. B is one of the reference surfaces (here the reference surfaces mean the parabolic OPDs of the imaginary ideal lenses, as Eq. (1)), and is coincident with the parabolic part of surface A. Many authors used B to get the expression of TL focal length [7,10–13]:

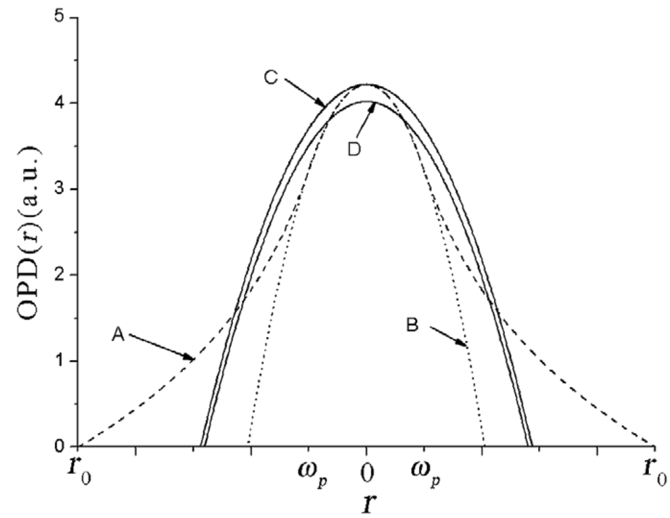

Fig. 1. An example of OPD distribution in the crystal and those of ideal lenses. A: An example of actual OPD; B, C, D: OPDs of the ideal lenses. B and C have the same OPD(0) and C and D have the same focal length.

$$f_\mathrm{T0} = \frac{\omega_\mathrm{pa}^2}{2A_0} \quad \text{(for “top-hat” pumping)}. \tag{6}$$

For Gaussian pumping, Eq. (A10) can be expanded into a power series. Only considering the r^2 term [2], the focal length was obtained as

$$f_\mathrm{T0} = \frac{\omega_\mathrm{pa}^2}{4A_0} \quad \text{(for Gaussian pumping)}. \tag{7}$$

These two equations are widely used for they are simple and convenient. And we call them the old expressions in this paper. Considering when an actual beam distribution is modeled as Gaussian or “top-hat”, the radius of the “top-hat” beam is $2^{-1/2}$ of that of the Gaussian beam, Eqs. (6) and (7) are substantially consistent with each other. Eqs. (6) and (7) were obtained using only the central part of the actual OPD or using only the r^2 term of the power series, they are precise enough only in the case of $\omega_\mathrm{l}^2 \ll \omega_\mathrm{p}^2$. But the pump radius is usually about the same as the laser mode radius, and the actual OPD is parabolic-logarithmic for “top-hat” pumping and nonparabolic for Gaussian pumping.

The difference between the actual OPD and that of an ideal lens is aberration. So according to the diffraction theory of the aberrations [18], the focus of the equivalent lens is the point of maximum normalized intensity, which can be estimated by the Strehl ratio weighted by $\exp(-r^2/\omega_\mathrm{l}^2)$ for TEM_{00} mode [19,20]:

$$\mathrm{SR} = \frac{\left|\int_0^{r_0} \exp\left\{-\mathrm{i}\frac{2\pi}{\lambda_\mathrm{l}}(\mathrm{OPD_A} - \mathrm{OPD_r})\right\}\exp\left(-\frac{r^2}{\omega_\mathrm{l}^2}\right)r\,\mathrm{d}r\right|^2}{\left|\int_0^{\infty}\exp\left(-\frac{r^2}{\omega_\mathrm{l}^2}\right)r\,\mathrm{d}r\right|^2}, \tag{8}$$

where λ_l is the wavelength of the laser; OPD_A is the $OPD(r) - OPD(0)$ caused by the actual thermal effect, corresponding to the OPD A in Fig. 1; OPD_r is the $OPD(r) - OPD(0)$ of the reference surface and is $-r^2/(2f)$, f is the focal length of ideal lens. Different reference surfaces result in different values of the SR.

C in Fig. 1 is the parabolic reference surface of the equivalent thermal lens. The $OPD(r) - OPD(0)$ of C is $-r^2/(2f_T)$, f_T is the actual TL focal length. Surface C and the value of f_T are gotten by making SR maximum. It is clear that any aberration from the reference surface will result in the diffraction loss. When the aberration is absent, the actual OPD is parabolic and the maximum value of SR is 1.

D in Fig. 1 is another parabolic surface with the same focal length with C, but different OPD(0), which means $OPD_C(r) - OPD_D(r)$ is a constant. It can be proved with Eq. (8) that the value of OPD(0) of the thermal lens will benefit nothing to the value of the Strehl ratio. This means it does not matter whether choosing C or D in Fig. 1 as the reference surface. Thus the only variable in Eq. (8) is the focal length. So we just need to find the right value of f_T to make SR maximum.

As Eq. (8) has no analytical solution, the numerical calculation has been done to find the correct values of f_T, which should make SR maximum. To make full use of the old equations which have been used for so many years and to accentuate the difference between the new and old values of the focal length, we give the calculation results by using a ratio r_f called correction factor, defined as the ratio of the new value of TL focal length to the old one, i.e.:

$$r_f = f_T/f_{T0}. \tag{9}$$

The numerical results are given as Fig. 2(a) and (b) for "top-hat" pumping and Gaussian pumping respectively. The correction factor is a function of ω_l/ω_{pa} and the larger ω_l is, the larger the correction factor is. When A_0 is smaller than 10^{-5} mm, the correction factor remains the same (upper line in Fig. 2(a) and (b)). When A_0 increases to 10^{-4} mm, the correction factor decreases a little (about 5%, lower line in Fig. 2(a) and (b)). And when A_0 is even larger, the correction factor is even smaller (not plotted), and the diffraction will be strong and may a circularly symmetric TEM_{10} mode or some higher mode oscillate, as observed in experiments in part IV. Also should be noted is that when the radius of the rod radius r_0 is large enough ($r_0 > 7\omega_{pa}$), the value of r_0 will not affect the value of the correction factor. Considering when an actual beam distribution is modeled as Gaussian or "top-hat", the radius of the "top-hat" beam is $2^{-1/2}$ of that of the Gaussian beam; Figs. 2, 3 will give results not far from each other. It is easy to understand the difference, as "top-hat" and Gaussian beam are different distribution, so the focal length for them should not be perfectly the same.

The expressions of the correction factor for $A_0 \leqslant 10^{-5}$ mm are given by curve fitting (x here is ω_l/ω_{pa}):

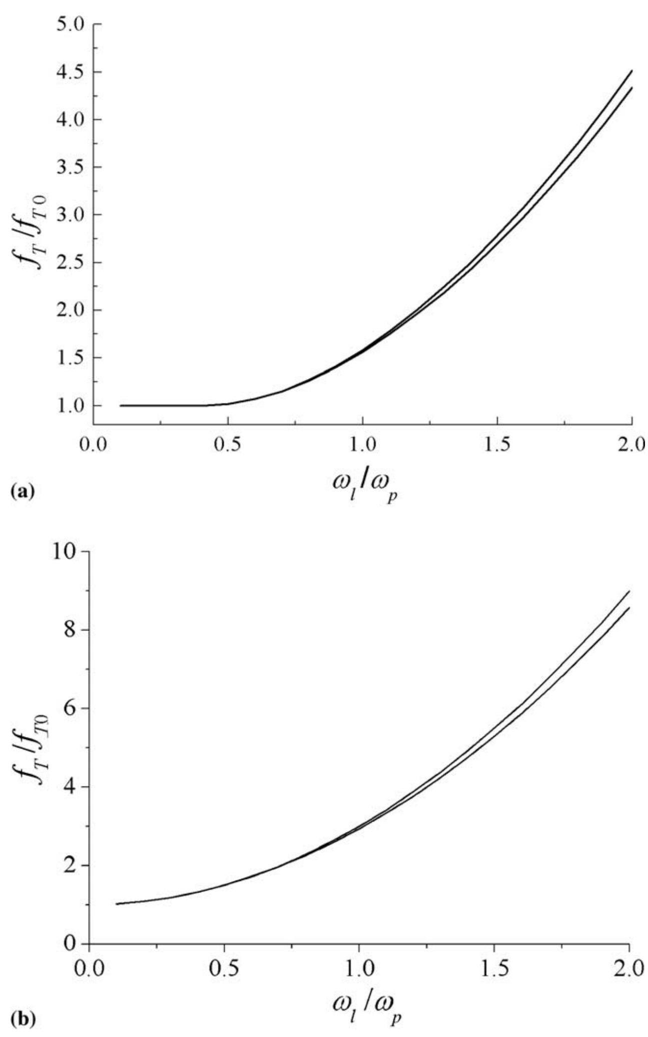

Fig. 2. The relationship of the new TL focal length and the old one under "top-hat" pump (a) and Gaussian pumping (b). Upper line: $A_0 \leqslant 10^{-5}$; lower line: $A_0 = 10^{-4}$.

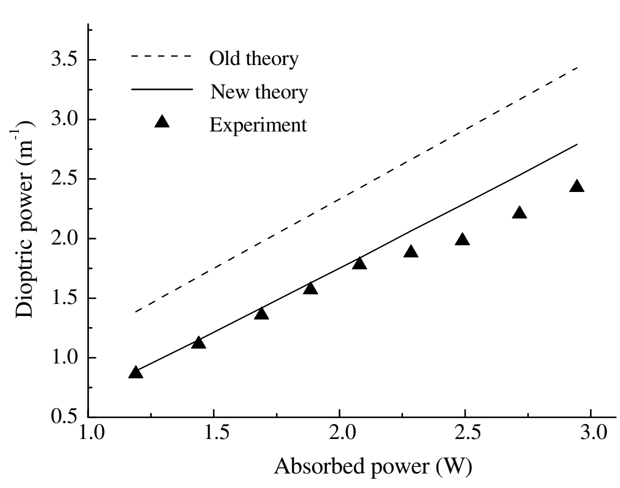

Fig. 3. Experimental results using the first LD pumping source with the cavity length 105 mm.

$$r_f(x) = 1.1 - 0.74x + 1.22x^2 \quad (2 > x \geqslant 0.4, \text{for "top-hat" pumping}), \tag{10}$$

$$r_f(x) = 1 + 2x^2 \quad (2 > x > 0, \text{for Gaussian pumping}). \tag{11}$$

Eqs. (11) and (12) can be used to estimate the focal length when A_0 is not very large (the error is small, when A_0 is larger than 10^{-5} mm and smaller than 10^{-4} mm). Note again that when $\omega_l/\omega_{pa} < 0.4$ for "top-hat" pumping, the old Eq. (6) or (7) can be used with good precision.

So the thermal focal length is (when $A_0 \leqslant 10^{-5}$ mm):

$$f_T = \frac{\omega_{pa}^2}{2A_0} \cdot \left[1.1 - 0.74\left(\frac{\omega_l}{\omega_{pa}}\right) + 1.22\left(\frac{\omega_l}{\omega_{pa}}\right)^2\right] \quad (2 > \omega_l/\omega_{pa} \geqslant 0.4, \text{for "top-hat" pumping}), \tag{12}$$

$$f_T = \frac{\omega_{pa}^2}{4A_0} \cdot \left[1 + 2\left(\frac{\omega_l}{\omega_{pa}}\right)^2\right] \quad (2 > \omega_l/\omega_{pa} > 0, \text{for Gaussian pumping}). \tag{13}$$

3. Analysis on average pump radius

If the pump radius cannot be approximated as a constant in the crystal, we divide the crystal into infinite slices and in each slice the pump radius can be considered as constant. The holistic focal lens is equivalent to these infinite thermal lenses are pressed together when the length of the cavity is much larger than that of the crystal. So the holistic focal length is [18]:

$$\frac{1}{f_T} = \int d\left(\frac{1}{f_T(z)}\right). \tag{14}$$

In the slice z to $z + dz$, the focal length satisfies the following relations:

$$d\left(\frac{1}{f_T(z)}\right) = d\left(\frac{1}{f_{T0}(z) \cdot r_f(\omega_l/\omega_p(z))}\right), \tag{15}$$

$$d\left(\frac{1}{f_{T0}(z)}\right) = \frac{2}{\omega_p^2(z)} \frac{A_0 \alpha e^{-\alpha \cdot z}}{1 - e^{-\alpha \cdot l}} dz \quad (\text{for "top-hat" pumping}), \tag{16}$$

$$d\left(\frac{1}{f_{T0}(z)}\right) = \frac{4}{\omega_p^2(z)} \frac{A_0 \alpha e^{-\alpha \cdot z}}{1 - e^{-\alpha \cdot l}} dz \quad (\text{for Gaussian pumping}). \tag{17}$$

We use $r_f(\omega_l/\omega_p(z))$ in this format ($x = \omega_l/\omega_p(z)$):

$$r_f(x) = C_a + C_b x + C_c x^2. \tag{18}$$

So Eq. (14) can be changed to:

$$1/f_T = \frac{2 \cdot A_0 \cdot \alpha}{1 - e^{-\alpha \cdot l}} \times \int_0^l \frac{e^{-\alpha \cdot z}}{C_a \omega_p^2(z) + C_b \omega_l \omega_p(z) + C_c \omega_l^2} dz \quad (\text{for "top-hat" pumping}), \tag{19}$$

$$1/f_T = \frac{4 \cdot A_0 \cdot \alpha}{1 - e^{-\alpha \cdot l}} \times \int_0^l \frac{e^{-\alpha \cdot z}}{C_a \omega_p^2(z) + C_b \omega_l \omega_p(z) + C_c \omega_l^2} dz \quad (\text{for Gaussian pumping}). \tag{20}$$

Comparing Eqs. (19) and (20) with Eqs. (12) and (13), the average pump radius can be gotten as

$$\frac{1}{C_a \omega_{pa}^2 + C_b \omega_l \omega_{pa} + C_c \omega_l^2} = \frac{\alpha}{1 - e^{-\alpha \cdot l}} \times \int_0^l \frac{e^{-\alpha \cdot z}}{C_a \omega_p^2(z) + C_b \omega_l \omega_p(z) + C_c \omega_l^2} dz. \tag{21}$$

Then the expressions (A4)–(A8) are substituted into Eq. (21) to get the average pump radius.

For Gaussian pumping, it is easy to give the analytical result:

$$\omega_{pa}^2 = \frac{1 - e^{-\alpha \cdot l}}{\alpha} \cdot \frac{\sqrt{m_1 \cdot m_2}}{\exp(-\alpha \cdot z_0) \cdot (a_1 \cdot b_2 + a_2 \cdot b_1)} - 2\omega_l^2 \quad (\text{for Gaussian pumping}), \tag{22}$$

where

$$m_1 = \frac{M^4 \lambda_p^2}{\pi^2 n^2 \omega_{p0}^2}, \quad m_2 = 2\omega_l^2 + \omega_{p0}^2, \tag{23}$$

a_1 and a_2 is the real and the image part of $\exp(i\alpha(m_2/m_1)^{1/2})$ respectively, and b_1 and b_2 is the real and the image part of $E_1(\alpha(l - z_0 + i(m_2/m_1)^{1/2})) - E_1(\alpha(-z_0 + i(m_2/m_1)^{1/2}))$ respectively.

When the laser is pumped by a "top-hat" beam, it is very difficult to give the analytical result for all the conditions as there is an absolute value calculation. So we only give the result when the pump beam waist is set on the input face of the crystal:

$$\omega_{pa} = \frac{\sqrt{4.4m_3 - 4.82} + 1.74\omega_l}{2.2} \quad (\text{for "top-hat" pumping}), \tag{24}$$

where,

$$m_3 = \frac{1 - e^{-\alpha \cdot l}}{\alpha} \frac{2.1955\omega_l \theta_p}{2(a_1 b_2 + a_2 b_1)}, \tag{25}$$

where a_1 and a_2 is the real and the image part of $\exp(\alpha m_4)$ respectively, and b_1 and b_2 is the real and the image part of $E_1(\alpha(l + m_4)) - E_1(\alpha m_4)$ respectively where

$$m_4 = \frac{2.2\omega_{p0} - 0.74\omega_l + i2.1955\omega_l}{2.2\theta_p}. \tag{26}$$

The exponential integral function (A11) is an existing program and runs fast in a normal personal computer. So Eqs. (22) and (24) provide a fast way to calculate the TL focal length.

4. Experimental evidence

We employed a plane–plane cavity using a ∅4 mm × 4 mm Nd:YAG crystal as the gain medium pumped by a fiber-coupled laser diode. As the laser beam radius changes along with the thermal lens when the pumping power changes, we can easily find the relation between the TL focal length and the laser beam radius. The output mirror is coated with reflectivity of 92% at 1064 nm. The rear mirror is the coating on the Nd:YAG. Two LDs coupled by different type of fibers are employed to obtain different pumping radii. The beam radii are measured by the knife edge method (KEM) and the focal lengths are calculated by using the beam radii at different positions. The average pump radius is estimated to be 0.35 mm and 0.30 mm for the first and the second LD used respectively. Calculations show that the average pump radius changes about ±5.0% and ±6.5% along with the laser radius for the first and the second LD respectively in the experiments. So we treat them as constants in calculations. Fig. 3 gives experimental results using the first LD pumping source with the cavity length of 105 mm. Figs. 4 and 5 give experimental results using the second LD pumping source with the cavity length of 105 mm and 220 mm respectively. Also the theoretical curves are presented to show the differences between the new theory, the old theory and the experiments. It can be seen from these figures that the new theoretical values are closer to the experiments than the old ones. The theoretical lines are calculated using the method provided in this paper and the ABCD law simultaneously. Fig. 6 gives dependence of the correction factor on the ratio of the laser radius to the pump radius. The solid triangles are experimental results calculated using the experimental results in Figs. 3–5. The line is obtained by using Eq. (10). It can be seen that the experimental and the theoretical results fit well. The parameters are taken from [21], as follows: $K = 10.46$ W/(Km), $\eta_h = 0.35$, $n = 1.82$, $\alpha = 2.85\ \mathrm{cm}^{-1}$, $\mathrm{d}n/\mathrm{d}T = 7.3\times10^{-6}\ \mathrm{K}^{-1}$, $\alpha_T = 7.5\times10^{-6}\ \mathrm{K}^{-1}$, $v = 0.3$, $C_r = 0.0195$. Note that the circularly symmetric TEM_{10} mode is observed when the pump power is increased, and an aperture in the cavity is used to limit the laser beam to be TEM_{00} mode.

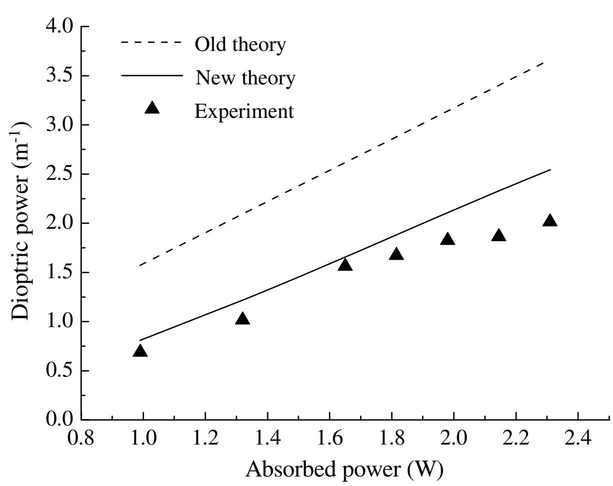

Fig. 4. Experimental results using the second LD pumping source with the cavity length 105 mm.

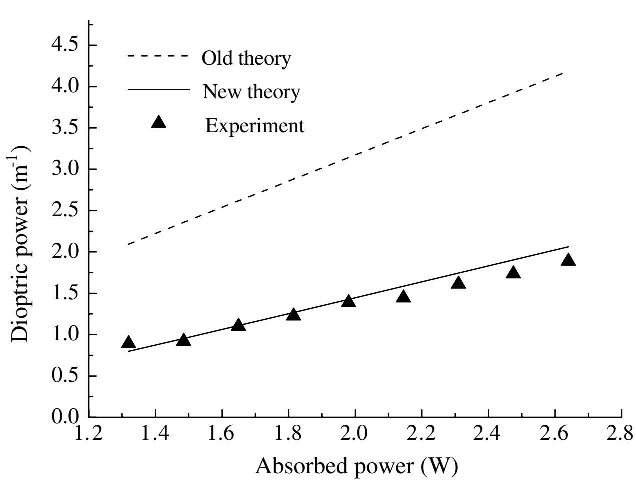

Fig. 5. Experimental results using the second LD pumping source with the cavity length 220 mm.

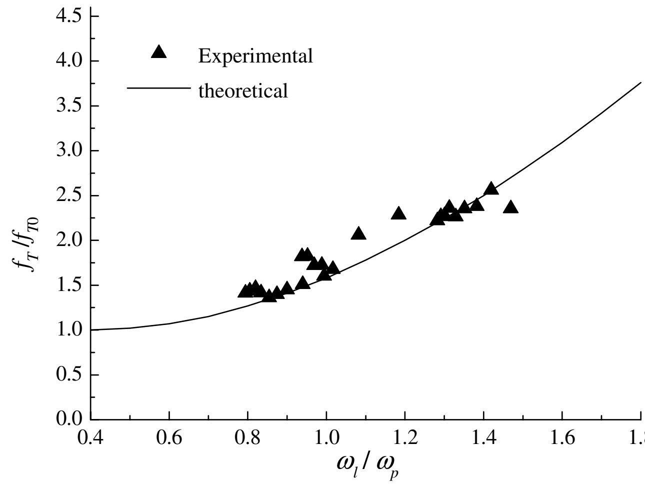

Fig. 6. Experimental and theoretical results of the correction factor.

5. Conclusion

A method of more precise determination of the focal length of equivalent thermal lens (TL) has been presented in this paper. The method is based on the diffraction theory of aberrations. By numerically calculating the optical path difference (OPD) distribution and the Strehl ratio, the focal lengths for "top-hat" pumping and Gaussian pumping have been obtained and the equations for the focal lengths have been presented by curve fitting. Also the equations for average pump radii have been presented. The experiment on a fiber-coupled LD pumped Nd:YAG laser has been carried out. The new result is closer to the experiment than the old theory.

Acknowledgements

This research is supported by the National Natural Science Foundation of China (No. 60478017), the Science and Technology Development Program of Shandong Province (No. 03BS095), and the Project-sponsored by SRF for ROCS, SEM.

Appendix A

The Poisson equation is usually used to describe the temperature distribution in the crystal in the classical theories. So the result only fits for continuously pumped solid-state lasers such as laser pumped or laser diode (LD) pumped ones. We consider that the heat flow is radial as the axial heat transfer coefficient on the two end faces is much smaller than the radial heat transfer coefficient on the side face (about one thousandth) [8]. And a constant-temperature boundary condition may be used as an excellent approximation. Considering with axisymmetric symmetry, the Poisson equation is as follow [3]:

$$\nabla^2 T(r,z) = -\frac{Q(r,z)}{K} = \frac{\partial^2}{\partial r^2}T(r,z) + \frac{1}{r}\frac{\partial}{\partial r}T(r,z), \tag{A1}$$

where $T(r,z)$ is the temperature distribution in Kelvin, $Q(r,z)$ is the heat source density that is a function of the pump power density, K is the heat conductivity in the solid, r is the radial coordinates.

The boundary condition is:

$$T(r_0,z) = T_0, \quad \left.\frac{\partial T(r,z)}{\partial r}\right|_{r=0} = 0, \quad \left.\frac{\partial T(r,z)}{\partial z}\right|_{z=0,l} = \infty, \tag{A2}$$

where T_0 is the temperature of the copper heat sink, r_0 is the radius of the rod, z is the axial coordinates.

The heat source in the crystal is a function of the pump power as $Q(r,z) = \eta_h \cdot P(r,z)$, where η_h is the fractional thermal load (the fraction of the absorbed pump power converted into heat). As is given by Fan [22], η_h can be written as

$$\eta_h = 1 - \eta_p\left[(1-\eta_l)\eta_r\frac{\lambda_p}{\lambda_f} + \eta_l\frac{\lambda_p}{\lambda_l}\right], \tag{A3}$$

where η_p is the pump quantum efficiency, the fraction of absorbed pumping photons contributing to inversion, η_r is radiative quantum efficiency for the upper level, the fraction of excited atoms that decay by a radiative path (not stimulated emission), η_l is the laser extraction efficiency, the fraction of excited ions that are extracted by stimulated emission, λ_p, λ_l are the wavelengths of pump light and stimulated emission respectively, and λ_f is the average wavelength of fluorescence photons. It should be noted that residual absorption of undoped crystal, multiphoton relaxation, concentration quenching could also be considered in this equation if necessary. The difference in lasing and nonlasing conditions results in different value of this equation.

We assume that the pump power experienced an exponential decay in the crystal, as the absorption saturation does not exist on most conditions. So the pump distributions are:

$$P(r,z) = P_{abs}\cdot p(r,z)\cdot\frac{\alpha}{1-e^{-\alpha\cdot l}}\cdot e^{-\alpha\cdot z}, \tag{A4}$$

where

$$p(r,z) = \frac{2}{\pi\cdot\omega_p^2(z)}\cdot\exp\left(-\frac{2r^2}{\omega_p^2(z)}\right) \quad \text{(for Gaussian beam)}, \tag{A5}$$

where

$$\omega_p^2(z) = \omega_{p0}^2\left\{1 + \left[\frac{M^2\cdot\lambda_p\cdot(z-z_0)}{\pi\cdot n\cdot\omega_{p0}^2}\right]^2\right\}, \tag{A6}$$

or

$$p(r,z) = \frac{1}{\pi\omega_p^2(z)}\Theta(\omega_p^2(z) - r^2) \quad \text{(for “top-hat” beam)}, \tag{A7}$$

where

$$\omega_p(z) = \omega_{p0} + \theta_p\cdot|z - z_0|, \tag{A8}$$

where $P(r,z)$ is the absorbed pump power distribution, $p(r,z)$ is the normalized pumping radiation distribution, P_{abs} is the total absorbed pump power, α is the absorption coefficient, l is the length of the rod, Θ is the Heaviside step function, $\omega_p(z)$ is the radius of pump beam at z, ω_{p0} is the waist radius of pump beam (to be consistent with the radius of electric field, this radius ω_{p0} and ω_l, which is the radius of laser beam, are defined as $1/e^2$ of the maximal intensity), n is the refractive index of the material, M^2 is the beam quality factor of the Gaussian pump beam, θ_p is the far-field half-angle of the “top-hat” beam, z_0 is the focal plane in the rod.

By substituting Eqs. (A3)–(A8) into Eq. (A1) and using Eq. (A2) as the boundary condition to solve the differential equation, the temperature distribution can be gotten as Eqs. (A9), (A10):

$$\begin{aligned}\Delta T(r,z) &= T(r,z) - T(r_0,z)\\ &= \eta_h\frac{P_{abs}}{4\pi K}\frac{\alpha e^{-\alpha\cdot z}}{1-e^{-\alpha\cdot l}}\left\{\left[1 - \frac{r^2}{\omega_p^2(z)} + \ln\left(\frac{r_0^2}{\omega_p^2(z)}\right)\right]\right.\\ &\quad\left.\times\Theta(\omega_p^2(z) - r^2) + \ln\left(\frac{r_0^2}{r^2}\right)\Theta(r^2 - \omega_p^2(z))\right\}\\ &\quad\text{(for “top-hat” pumping)},\end{aligned} \tag{A9}$$

$$\begin{aligned}\Delta T(r,z) &= T(r,z) - T(r_0,z)\\ &= \eta_h\frac{P_{abs}}{4\pi K}\frac{\alpha e^{-\alpha\cdot z}}{1-e^{-\alpha\cdot l}}\left[\ln\left(\frac{r_0^2}{r^2}\right) + E_1\left(\frac{2r_0^2}{\omega_p^2(z)}\right) - E_1\left(\frac{2r^2}{\omega_p^2(z)}\right)\right]\\ &\quad\text{(for Gaussian pumping)},\end{aligned} \tag{A10}$$

where E_1 is the exponential integral function defined as

$$E_1(x) = \int_1^\infty \frac{e^{-xt}}{t}\,dt. \tag{A11}$$

References

[1] W. Koechner, Appl. Opt. 9 (11) (1970).
[2] M.E. Innocenzi, H.T. Yura, C.L. Fincher, R.A. Fields, Appl. Phys. Lett. 56 (19) (1990) 1831.

[3] W. Koechner, Solid-state laser engineering, in: Arthur L. Schawlow (Ed.), Springer Series in Optical Sciences, Springer, Berlin, 1999, fifth revised and updated edition.
[4] F. Song, C. Zhang, X. Ding, J. Xu, G. Zhang, Appl. Phys. Lett. 81 (12) (2002) 2145.
[5] R. Weber, B. Neuenschwander, M. MDonald, M.B. Roos, H.P. Weber, IEEE J. Quantum Electron. 34 (6) (1998) 1046.
[6] P.K. Mukhopadhyay, A. Nautiyal, P.K. Gupta, K. Ranganathan, J. George, S.K. Sharma1, T.P.S. Nathan, Appl. Phys. B 77 (1) (2003) 81.
[7] W.A. Clarkson, J. Phys. D: Appl. Phys. 34 (16) (2001) 2381.
[8] A.K. Cousins, IEEE J. Quantum Electron. 28 (4) (1992) 1057.
[9] A.K. Cousins, Appl. Opt. 31 (34) (1992).
[10] S. Chénais, F. Balembois, F. Druon, G. Lucas-Leclin, P. Georges, IEEE J. Quantum Electron. 40 (9) (2004) 1217.
[11] Y.P. Lan, Y.F. Chen, S.C. Wang, Appl. Phys. B 71 (1) (2000) 27.
[12] Y.F. Chen, J. Opt. Soc. Am. B 17 (11) (2000) 1835.
[13] W.J. Xie, S.C. Tam, Y.L. Lam, K.S. Lai, R.F. Wu, Y.L. Lim, E. Lau, IEEE J. Quantum. Electron. 37 (10) (2001) 1368.
[14] J.A. Zheng, S.Z. Zhao, L. Chen, Opt. Laser Tech. 34 (6) (2002) 439.
[15] Y.F. Chen, personal communication.
[16] A. Agnesi, P. Uggetti, Opt. Comm. 212 (6) (2002) 371.
[17] C. Pfistner, R. Weber, H.P. Weber, S. Merazzi, R. Gruber, IEEE J. Quantum Electron. 30 (7) (1994) 1605.
[18] M. Born, E. Wolf, Principles of Optics, sixth ed., Pergamon Press, Oxford, U.K, 1980.
[19] V.N. Mahajan, J. Opt. Soc. Am. 71 (1) (1981) 75.
[20] Y.F. Chen, T.M. Huang, C.F. Kao, C.L. Wang, S.C. Wang, IEEE J. Quantum Electron. 33 (8) (1997) 1424.
[21] H. Glur, R. Lavi, T. Graf, IEEE J. Quantum Electron. 40 (5) (2004) 499.
[22] T.Y. Fan, IEEE J. Quantum Electron. 29 (6) (1993) 1457.